

# A Foreign Object Damage Event Detector Data Fusion System for Turbofan Engines

James A. Turso\*  
*QSS Group, Inc., Cleveland, OH 44135*

and  
Jonathan S. Litt†  
*U. S. Army Research Laboratory, Glenn Research Center, Cleveland, OH 44135*

A Data Fusion System designed to provide a reliable assessment of the occurrence of Foreign Object Damage (FOD) in a turbofan engine is presented. The FOD-event feature level fusion scheme combines knowledge of shifts in engine gas path performance obtained using a Kalman filter with bearing accelerometer signal features extracted via wavelet analysis to positively identify a FOD event. A fuzzy inference system provides basic probability assignments based on features extracted from the gas path analysis and bearing accelerometers to a fusion algorithm based on the Dempster-Shafer-Yager Theory of Evidence. Details are provided on the wavelet transforms used to extract the foreign object strike features from the noisy accelerometer data and on the Kalman filter-based gas path analysis. The system is demonstrated using a turbofan engine combined-effects model, providing both gas path and rotor dynamic structural response, which is suitable for rapid-prototyping of control and diagnostic systems. The fusion of the disparate data can provide significantly more reliable detection of a FOD event than the use of either method alone. The use of fuzzy inference techniques combined with Dempster-Shafer-Yager Theory of Evidence provides a theoretical justification for drawing conclusions based on imprecise or incomplete data.

## Nomenclature

$A$	state space model system matrix, fused event set
$A_i$	source $i$ event set
$BE$	belief
$\delta$	deviation from steady state operating condition
$f$	frequency in Hz
$m$	basic probability assignments (bpa)
$PROB$	probability
$PL$	plausibility
$\delta\hat{x}, \delta\hat{y}, \delta\hat{h}$	estimated state variables, output, and health parameters
$Y(f)$	discrete Fourier transform of $y(n)$
$\varphi$	null set

---

Presented as Paper 2004-4047 at the AIAA Joint Propulsion Conference and Exposition, Ft. Lauderdale, FL, 11–14 July 2004; received 20 July 2004; revision received 8 April 2005; accepted for publication 14 May 2005. This material is declared a work of the U.S. Government and is not subject to copyright protection in the United States. Copies of this paper may be made for personal or internal use, on condition that the copier pay the \$10.00 per-copy fee to the Copyright Clearance Center, Inc., 222 Rosewood Drive, Danvers, MA 01923; include the code 1542-9423/04 \$10.00 in correspondence with the CCC.

\* Senior Research Engineer, Controls and Dynamics Branch, NASA Glenn Research Center, 21000 Brookpark Road MS 77-1. AIAA Member.

† Aerospace Engineer, Vehicle Technology Directorate, NASA Glenn Research Center, 21000 Brookpark Road M.S. 77-1. AIAA Member.

## I. Introduction

Although ingestion of birds and ice has occasionally resulted in uncontained rotor events in commercial jet transport,<sup>1</sup> in the vast majority of cases bird ingestion does not affect the safe outcome of a flight and may, in fact, go unnoticed by the flight crew.<sup>2</sup> However ingestion does pose a risk of Foreign Object Damage (FOD), and even in a case where there is no apparent damage to an engine as observed from the cockpit, latent effects (e.g. cracks that can be propagated by high cycle fatigue<sup>3</sup>) may be present; thus it is important to be aware of its occurrence, if possible. However, there is currently no automatic detection of foreign object ingestion performed on aircraft engines. A system that detects foreign object impact has two potential uses, depending on the level of certification achievable. The first, and simplest to implement from a certification standpoint, reports to the ground crew that a foreign object was ingested and initiates a maintenance action. The second is harder to certify because it requires providing an indicator to the pilot, but is potentially more beneficial from a safety point of view because it addresses the issue of pilot response to an event. This use is suggested by the numerous cases of bird ingestion contributing to accidents, some of them fatal.<sup>4</sup> Specific pilot procedures have been developed for situations where ingestion is suspected, and forensic analysis has repeatedly shown that they would have been the appropriate actions to take in cases where rejected takeoffs motivated by bird ingestion resulted in accidents.<sup>5</sup> When a multi-engine aircraft flies through a flock of birds, potentially damaging more than one engine, the pilot needs to understand the status since his resulting actions may be different depending on the number of engines involved. Most FOD events occur close to the ground when the flight crew's attention is focused on flying the plane. Only after the crew stabilizes the aircraft at a safe altitude should they take action on the engine.<sup>2,5</sup> This specifically applies to cases where ingestion is suspected but no serious damage is obvious. Specific pilot actions may be called for in cases where engine fire, severe damage, or separation is evident. Once the aircraft is stable, the reduced workload in the cockpit environment provides better circumstances under which the crew can analyze the situation, and they would benefit greatly by having full knowledge of the engines involved and the likelihood of the event based on data, and this is the type of information such a system could provide. Either of these two uses provides justification for the development of a FOD detection system. This paper will not address how the system should be used beyond this; the objective was to make the reader aware of the utility such a system can provide.

The critical consequence of foreign object ingestion is engine surge, potentially resulting in the loss of power. The flight crew can recognize foreign object ingestion through a combination of instrument readings and sensory cues. These include such symptoms as a thud or bang, a fire warning, a visible flame coming out of the engine, vibration, yaw of the airplane caused by thrust imbalance, high Exhaust Gas Temperature (EGT), change in the spool speeds, smoke/odor in cabin bleed air, and Engine Pressure Ratio (EPR) change. It is important to note that for impact-type FOD (due to ice, birds, runway debris, etc.), the damage is primarily to the fan and front part of the engine, with the extent of the damage determined by the geometry, angle of impact, hardness, relative speed, etc. of the object. This is quite different from ingestion of volcanic ash, which may severely affect the hot section of the engine while producing no visible damage to the cooler portions in the front.<sup>6</sup>

Given that many of the potential symptoms of FOD are not unique to that event, an automatic system for FOD detection should take information from multiple sources to provide confidence in its diagnosis. Just like a pilot does, this system must fuse the information in a way that provides a measure of the likelihood of foreign object ingestion in order to determine any corrective action. Additionally, since several of the potential symptoms are described in terms of human senses, alternate information sources need to be developed, and they should utilize the standard engine sensor suite (or a very similar suite) to address issues such as certification and retrofit. Naturally the processing requirements may vary from the current systems simply due to the fact that additional signal processing is being added to execute these algorithms on line. Some testing has been carried out with an Ingested Debris Monitoring System (IDMS), but it is still considered an immature technology<sup>7</sup> and is not a candidate for retrofit.

Effective diagnostic system development requires identification and extraction of the essential signal features necessary for a timely, accurate assessment of the state of the system being monitored. For a given malfunction or event (e.g., a FOD event) this requires identification of the key components affected by the event, the parameters and appropriate signals to be analyzed, and the essential features within the signals that provide the minimum information necessary to arrive at a diagnosis, i.e., *reduction of the dimensionality of the raw data*. In this work

we address impact-type events and have chosen to fuse data from a Gas Path Analysis (GPA) with rotordynamic structural effects to provide an indication of the presence of FOD. Gas path and structural data are fused because the general responses to foreign object ingestion are known for each system though neither alone is sufficient to uniquely diagnose it, both systems are monitored already so existing instrumentation may be sufficient for the task, and it builds upon existing experimental work in the two areas individually. Changes in component efficiencies, high and low spool speeds, as well as changes in other engine parameters have been determined/observed using data from FOD tests.<sup>8,9</sup> In some cases, these parameter changes alone may not be conclusive proof that a FOD event has occurred. Incorporation of structural vibration signals provides a means to aid in positive identification of a FOD event. To successfully apply available sensor fusion techniques, the same event should be detected using sensors that have significantly different physical characteristics (e.g., thermocouples compared to accelerometers) and rely on measuring physically different parameters (e.g., temperature vs. acceleration).<sup>10,11</sup> Fusing gas path performance parameter estimates with structural response information acquired during a FOD event could provide conclusive evidence that a FOD event had occurred. For example, model mismatch or sensor bias<sup>12</sup> could conceivably result in gas path performance parameter estimate changes similar to those experienced during a FOD event. Similarly, vibration signals alone may possess FOD-like characteristics depending on the maneuver, e.g., a rapid change in thrust demanded from the engine would result in temporary impulse-like force imbalances which are transmitted through the engine structure. The combination of available evidence, i.e., specific changes in gas path performance parameter estimates combined with application of state-of-the-art signal processing techniques applied to structural vibration signals (e.g., wavelet analysis<sup>13,14</sup>), could provide the “fingerprint” necessary to positively identify a FOD event. In the present investigation we are detecting impact events, so we assume that the component most affected by a FOD event in a turbofan engine is the fan, with any damage incurred resulting in changes in fan efficiency and efficiency rate of change.<sup>9</sup> Fan structural changes resulting from a FOD event could manifest themselves as abrupt, short duration changes in the vibration signal due to the object’s impact upon the fan disk, extracted using wavelet analysis, as well as changes in the amplitude of vibration and the amplitude of vibration rate of change due to FOD event-induced rotor imbalance.

This paper describes the proof-of-concept development and application of a FOD event detection scheme, utilizing features extracted from rotor structural data (accelerometer signals) and analytical measurements (gas path analysis). Figure 1 provides an overview of the fusion system. The vibration data-driven portion of the system utilizes a wavelet-based algorithm developed as part of the work presented in Ref. 15. Selected features are extracted from the gas path analysis and the engine’s vibration monitoring system and assessed via two fuzzy inference engines respectively, each providing a “possibility” distribution for FOD event occurrence. The inference engines (or “experts” used in the present context) assign degrees of membership to these features, which are subsequently transformed into basic probability assignments for the gas path and vibration components, and are fused via Dempster’s combination algorithm.<sup>16</sup> The features being categorized in the gas path analysis are fan efficiency and time rate-of-change of fan efficiency. For the vibration component, the acceleration signals are processed using a wavelet transform-based algorithm, with a new wavelet being created for the specific purpose of finding abrupt changes in noisy accelerometer signals due to FOD events. Two additional features extracted are the amplitude of vibration (determined via a single-frequency Fourier transform calculated at the rotational speed of the engine), and the rate-of-change in amplitude due to a FOD-induced rotor imbalance. The system developed fuses information at the *feature level*<sup>17</sup> and is intended to provide a reduced information set to a decision maker, i.e., the *decision level fusion*.

The paper is organized as follows. Following the parallel paths shown in Fig. 1, Section II provides a description of hypothesized FOD event effects on the gas path analysis and structural response of a (simulated) turbofan engine as well as the techniques used to extract selected features from the gas path analysis and vibration signals. The bottom box of Fig. 1 encompasses Section III, which describes the method used for basing a decision (e.g., whether or not a FOD event has occurred) on imprecise, uncertain information from multiple sources, i.e., the features extracted from the gas path analysis and vibration signals. Details of the fuzzy inference engines (one for each expert) and fusion algorithm are provided. Section IV presents the results for three cases where: 1) the experts are in perfect agreement that a FOD event has occurred, 2) the information extracted leads to uncertainty in the fused, final conclusion, and 3) the evidence presented leads to direct conflict among the experts. An alternate method for presenting the fused information is also presented. Conclusions are provided in Section V.

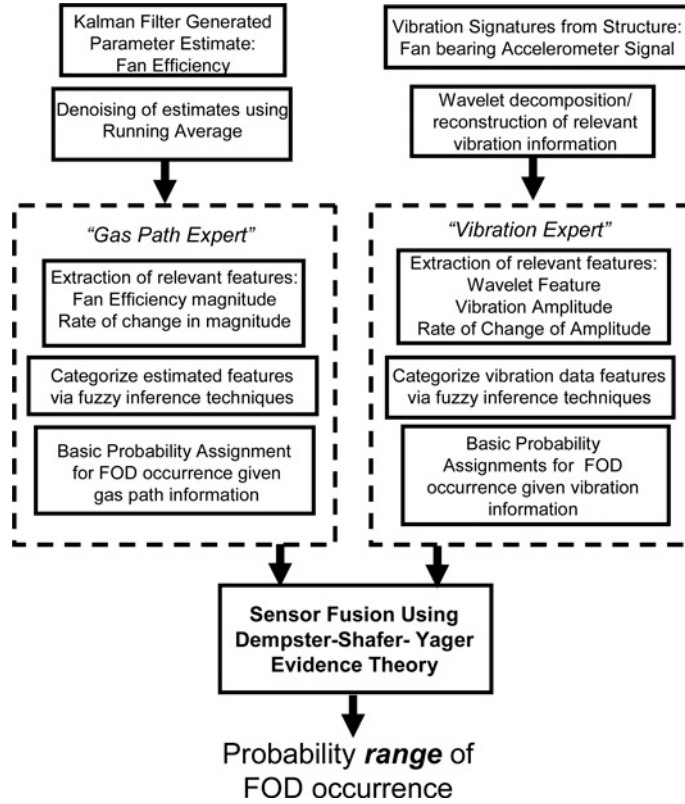


Fig. 1 FOD-event Gas Path Analysis/Structural Response Evidence Fusion Architecture.

## II. Signal Conditioning and Feature Extraction from Gas Path and Vibration Sensor Measurements

### A. Gas Path Analysis Feature Extraction via Kalman Filter Estimation

For approximately two decades techniques based on the Kalman filter<sup>18</sup> (Fig. 2) have been applied to turbofan engine diagnostics.<sup>19,20</sup> Specifically, Kalman filters have been used for detection of engine degradation via estimation of a set of health parameters—parameters that give an indication of the health of the engine—which are in general not measurable themselves (e.g., compressor or fan efficiency), but are calculated via knowledge of measurable quantities. The degradation monitored may be gradual in nature, e.g., worn components result in increased internal clearances resulting in decreased component efficiency, or may be due to an abrupt event as is the case when foreign objects are ingested into the engine. Because the Kalman filter uses gas path measurements in its computations, it implicitly fuses some of the same data a pilot uses to diagnose a FOD event.

A state-variable model of the engine is used in the estimator as part of the on-board diagnostic system. The linearized model of the engine has the form

$$\begin{aligned} \delta\dot{x} &= A\delta x + B\delta u + L\delta h \\ \delta y &= C\delta x + D\delta u + M\delta h \end{aligned} \tag{1}$$

where  $\delta x$ ,  $\delta y$ , and  $\delta u$ , are deviations in the state, output, and input vectors, respectively, and  $\delta h$  represents the vector of health parameter shifts caused by degradation.  $A$ ,  $B$ ,  $C$ ,  $D$ ,  $L$ , and  $M$  are matrices of appropriate dimension.

When using the Kalman filter as a health parameter estimator, the health parameters are interpreted as additional state variables to be estimated. These additional state variables are typically assumed to be constant (no dynamics), thus the corresponding entries in the system matrix of the state-space system representation are zero. The resulting

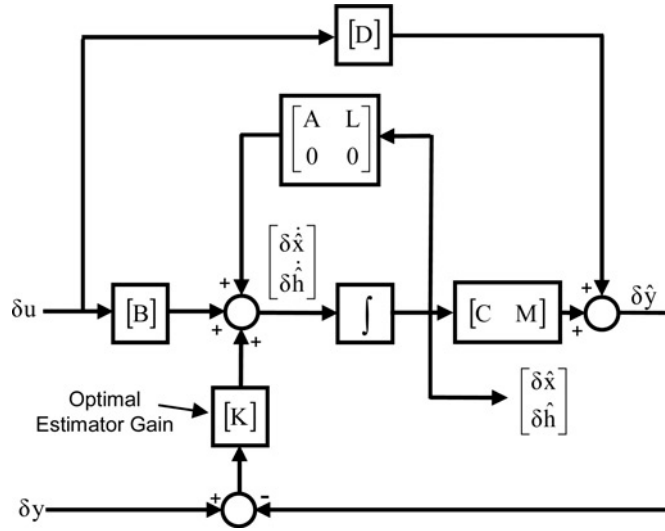


Fig. 2 Overview of the Kalman Filter parameter estimator.

state space representation is

$$\begin{bmatrix} \delta \dot{x}(t) \\ \delta \dot{h}(t) \end{bmatrix} = \begin{bmatrix} A & L \\ 0 & 0 \end{bmatrix} \begin{bmatrix} \delta x(t) \\ \delta h(t) \end{bmatrix} + \begin{bmatrix} B \\ 0 \end{bmatrix} \delta u(t)$$

$$\delta y(t) = \begin{bmatrix} C & M \end{bmatrix} \begin{bmatrix} \delta x(t) \\ \delta h(t) \end{bmatrix} + D \delta u(t)$$

with  $[\delta x(t)^T \delta h(t)^T]^T$  referred to as the *augmented* state vector. The specific health parameter (or parameters) used by the fusion system is dictated by the component (or components) most likely to be affected by a FOD event. It has been shown that fan efficiency and fan flow capacity are likely to be affected immediately by a FOD event<sup>8</sup> and thus foreign object ingestion is modeled as abrupt health parameter shifts in the GPA literature.<sup>12,21</sup> Thus, for the present investigation, fan efficiency is the health parameter of interest. We assume that the larger the impact, the larger the deviation in the health parameter values. The features extracted from the efficiency estimate are the *denoised* versions of the estimated fan efficiency and the rate-of-change of the fan efficiency. For a FOD event, significant changes in the efficiency and rate-of-change in efficiency are expected to be coincident. Figure 3 presents an example of the estimated efficiency, which shows the effect of sensor noise on the estimate. The other feature used by the fusion system, rate of change of efficiency, requires taking the derivative of a noisy signal, which results in an amplification of the noise rendering this feature unusable in the present context. Thus, a means is required for effectively denoising the efficiency estimate prior to calculating its rate of change. Figure 3 also shows the efficiency estimate after denoising using a running average. The noise level is significantly decreased, which allows for easier detection of significant changes in the efficiency rate-of-change. The time lag introduced by the running average (approximately 0.5 seconds) is considered acceptable given the present application, with the tolerable time lag ultimately dictated by the end use of the system.

**B. Vibration Signal Feature Extraction**

Much of the specific information concerning the vibration signatures associated with FOD events (e.g., rotor frequencies excited during foreign object impact on the fan disk) in turbofan engines is not available in the open literature. Also, analytical structural models of aircraft engines, such as Finite Element Models (FEMs), are typically computationally intensive due to the vast amounts of time-dependant spatial data they produce, and do not lend themselves for direct application to diagnostic system development and testing.<sup>15</sup> Due to the lack of high-frequency FOD event test data in the open literature, a Reduced-Order turbofan structural Model (ROM) was synthesized from

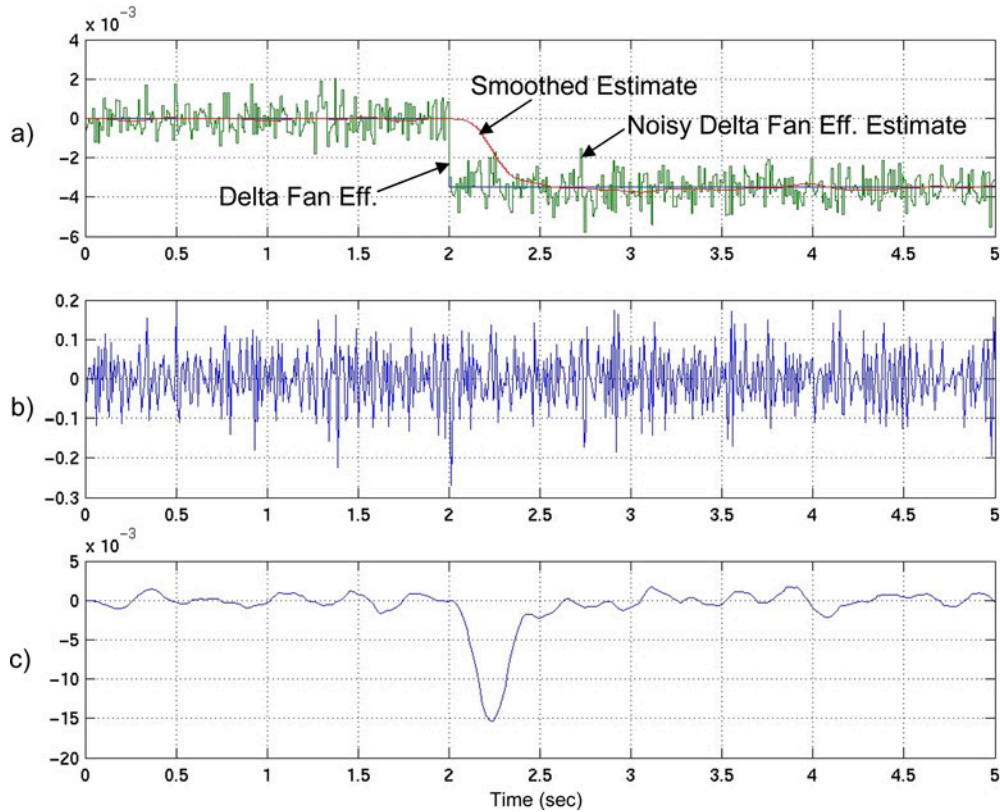


**Fig. 3 a) Kalman Filter delta fan efficiency estimate, actual delta efficiency, and smoothed estimate, b) rate-of-change of delta fan efficiency estimate prior to smoothing, c) rate-of change of delta fan efficiency estimate based on smoothed delta efficiency estimate.**

a finite element model modal analysis of the rotor assembly of a large turbofan jet engine to support this investigation. The resulting ROM transient response was benchmarked against the finite element code and considered to be adequate for the present investigation. Use of the ROM provided a factor of 40 decrease in run time compared to the FEM, which correspondingly decreased the development time of the fusion system. An example transient response from an inherent rotor imbalance and FOD of the turbofan model (exaggerated to highlight the effects) is shown in Fig. 4. A rotor vibration sensor signal measured at the fan bearing (a typical location on a turbofan engine) during a FOD event would consist of the response of a dominant low-frequency lateral mode excited from an impulsive moment at the fan disk/rotor shaft due to the initial impact of the foreign object upon the fan disk. Higher frequency lateral modes would also be excited due to the high frequency content of the foreign object impact, and appear in the sensor signal immediately after the event. Possible longer lasting effects due to resulting permanent blade damage, i.e., an imbalance force occurring at a frequency corresponding to once per revolution of the rotor, may also appear. Rotating equipment tends to have a relatively small degree of inherent imbalance after manufacturing<sup>22</sup> which is also included in the reduced order structural model for a “steady state” response. The FOD-event depicted in Fig. 4 produces no permanent imbalance (structural damage). A permanent imbalance would have resulted in increased steady-state amplitude after the FOD event. The hypothesized sequence of events is predominantly based on intuition and qualitative assessments by the authors.

Consider the simulated bearing accelerometer signals shown in Fig. 5. At 3.44 seconds, a 0.5 lbm foreign object hits the fan disk with a speed of 300 mph at a radius of 20 inches. The event is modeled as a pulse of width 0.05 seconds, with a magnitude determined using the method presented in Ref. 15. A fan disk eccentricity of 0.001 inches is assumed. The event results in no additional permanent imbalance. As shown in Fig. 5a, the event is barely noticeable

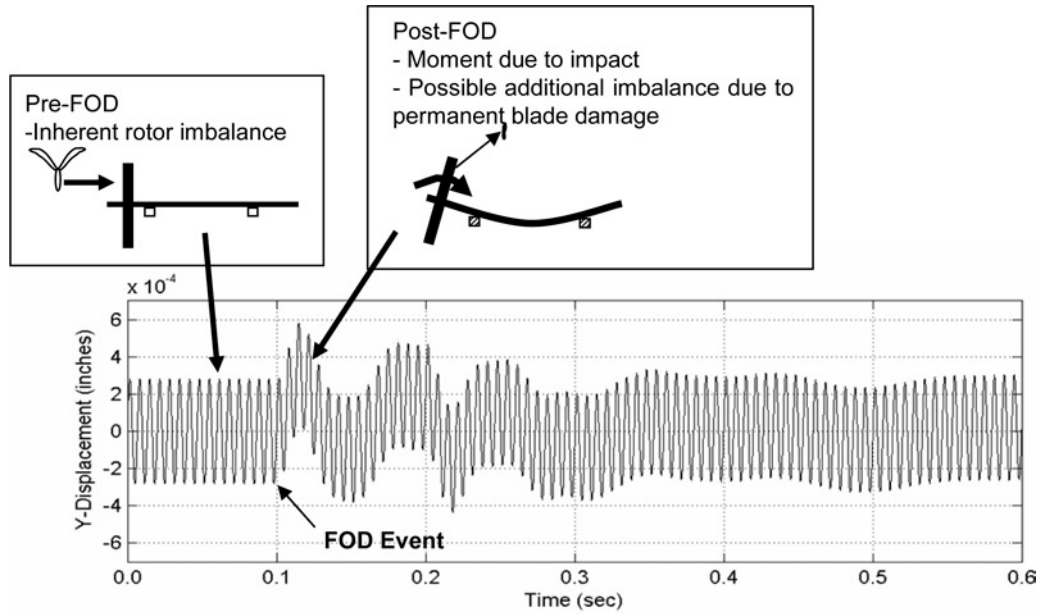


**Fig. 4 Representative response at bearing location to a moderately-sized FOD event.**

in the time trace for a noise-free situation. However accelerometer signals on in-service engines are typically noisy. In addition to “process noise,” i.e., random motion of the aircraft due to wind gusts and compensating maneuvers being transmitted from the airframe to the engine, there is a significant amount of sensor noise which may mask the occurrence of a FOD event. Figure 5b shows the noise-corrupted bearing accelerometer signal with a signal-to-noise

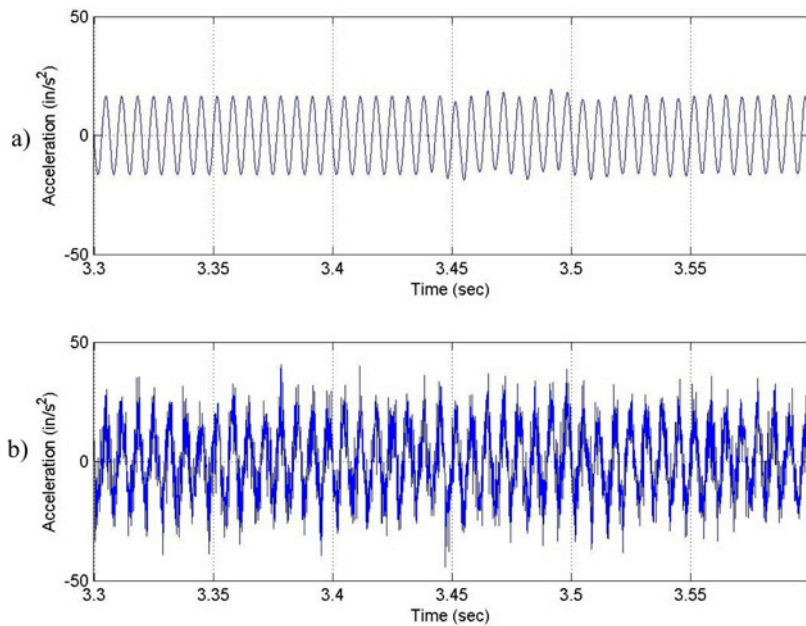


**Fig. 5 Bearing Accelerometer output signal corresponding to a FOD event. a) Noise free system response. b) System response with process and sensor noise.**

ratio of approximately 3.5 (11 dB). Observation of the signal shows no well-defined point in time at which one would identify a FOD event occurrence. Had there been permanent imbalance, the event may have been detected by the increased amplitude of vibration (this is the type of information available in current vibration monitoring systems). However, if no additional permanent imbalance is induced, this would be among the most difficult scenarios to detect for a diagnostic system, and highlights the need for an additional feature to be extracted from the signal which can effectively identify the abrupt change at the time of a FOD event. Wavelet decomposition, reconstruction, and conditioning will provide this additional feature.<sup>23,24</sup>

**C. FOD Event Detection Using Wavelet Analysis of Rotor Bearing Vibration Signals**

Over the past decade the discrete time wavelet transform (DTWT) has been applied to a wide range of signal analysis problems, e.g., de-noising of signals as well as time localization and reconstruction of short duration changes.<sup>14,23,24</sup> The DTWT has been shown to be a viable candidate for the present study due to the nature of the signal characteristic of interest, i.e., an abrupt change in a bearing vibration signal due to a FOD event, corrupted by noise.<sup>15</sup> The details of the technique are shown in Ref. 15 and are only summarized here.

Mallett<sup>25</sup> proposed a technique for identifying a wavelet specifically designed for edge detection. A signal is passed through a smoothing function (e.g., a low pass filter) and differentiated multiple times. The combination of smoothing and differentiation results in a wavelet customized to the application. This technique was adapted to identify the FOD event-induced short-time change in accelerometer signals. The smoothing filter chosen for the present investigation is the Daubechies 8 wavelet decomposition. As shown in Fig. 6, the accelerometer signal is passed through an approximation filter bank three times and subsequently passed through a detail filter. This provides a means to focus on a *subband* of the original signal where the feature of interest is thought to lie, the

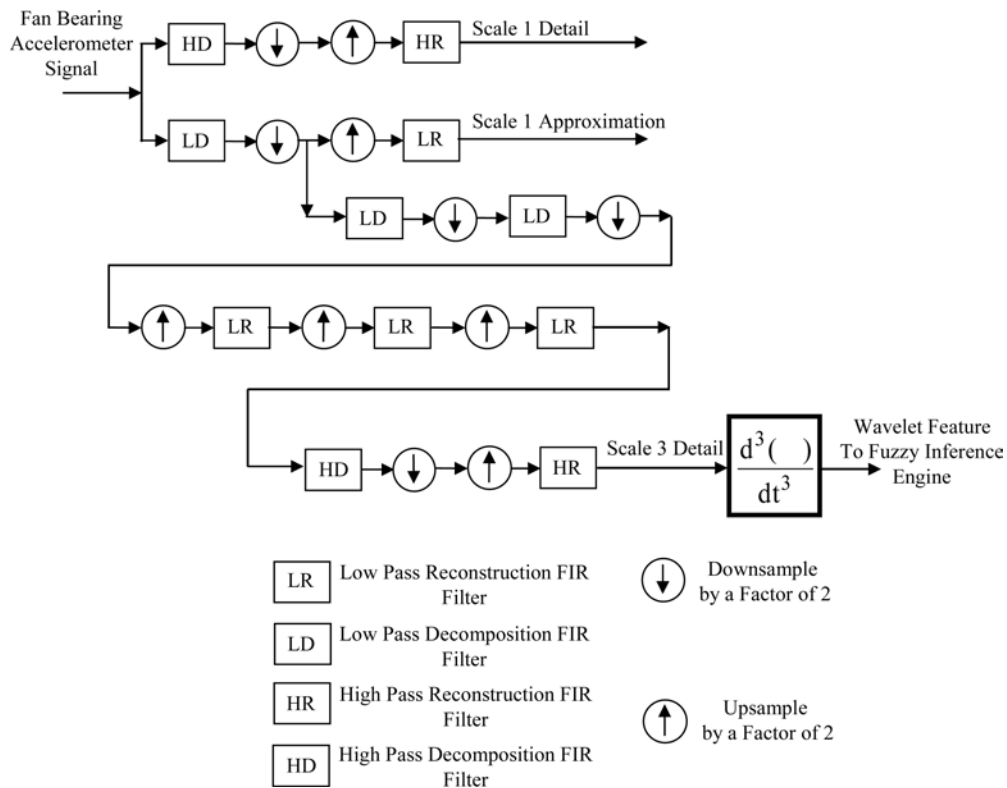


**Fig. 6 Wavelet transform-based vibration feature extraction implemented using an analysis and synthesis FIR filter bank.**



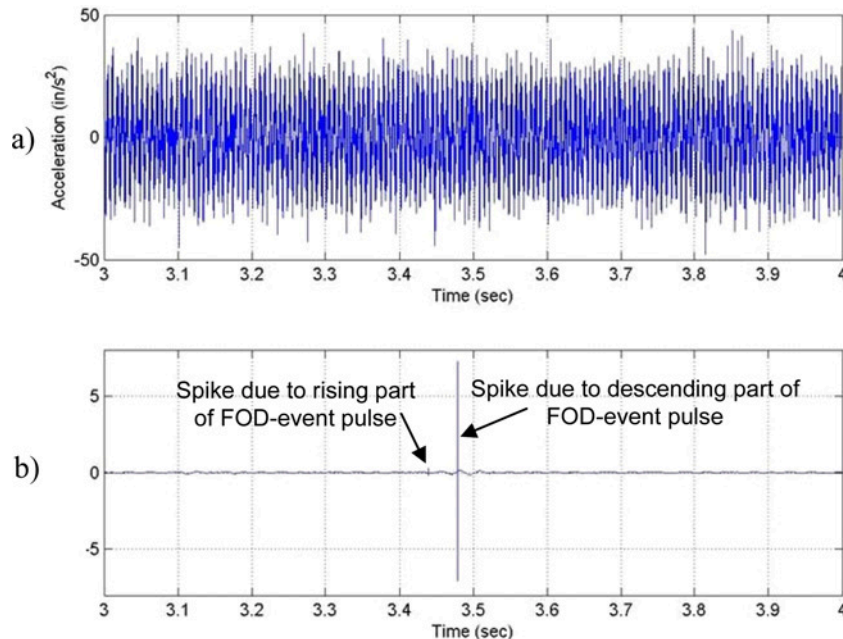
net effect being a low-pass filtering or smoothing operation. The result is differentiated three times to produce the feature used by the *structural expert* (i.e., structural component fuzzy inference engine) in the next step of the fusion process.

Figure 7 presents the wavelet decomposition of an accelerometer signal, a portion of which is shown in Fig. 5, using the custom wavelet described above. The exact time of the event is precisely determined using this technique. Indeed, the event is modeled by imposing a pulse whose magnitude is a function the of foreign object impact characteristics presented in Ref. 15 on the fan disk. The two spikes shown in Fig. 7 result from the rising and descending parts of that pulse “filtered” through the mechanical (i.e., rotor-bearing) system. The *event input profile* to the model (i.e., the pulse input described above) was considered to be appropriate for a significant, *structurally damaging* event, i.e., where the foreign object absorbs virtually none of the energy of impact, resulting in complete and immediate transfer of energy to the fan disk. This would be the case for hard objects such as ice, for example. For other scenarios, pulses of lower magnitude or with non-infinite rising (or descending) slopes may require higher-order differentiation for detection.

If a permanent imbalance results from a FOD event, two other features extracted from the accelerometer signal may assist in the diagnosis. These are the vibration amplitude and rate-of-change of amplitude determined from the magnitude of a single-frequency discrete Fourier transform,<sup>26</sup>

$$Y(f) = \sum_{n=-\infty}^{\infty} y(n)e^{-j2\pi fn}$$

The analysis frequency corresponds to the rotational speed of the rotor and would practically be obtained from a once-per-revolution signal used to gauge engine rotational speed. Large amplitudes accompanied by high amplitude-rates-of-change would be indicators that a FOD event has occurred. An example of the three features obtained from the fan bearing accelerometer signal is shown in Fig. 8 for a simulated FOD event (using the combined-effects model mentioned earlier) at 2.0 seconds.



**Fig. 7** Noisy bearing accelerometer signal analyzed using custom wavelet a) accelerometer signal b) Wavelet Feature extracted identifying time of impact.

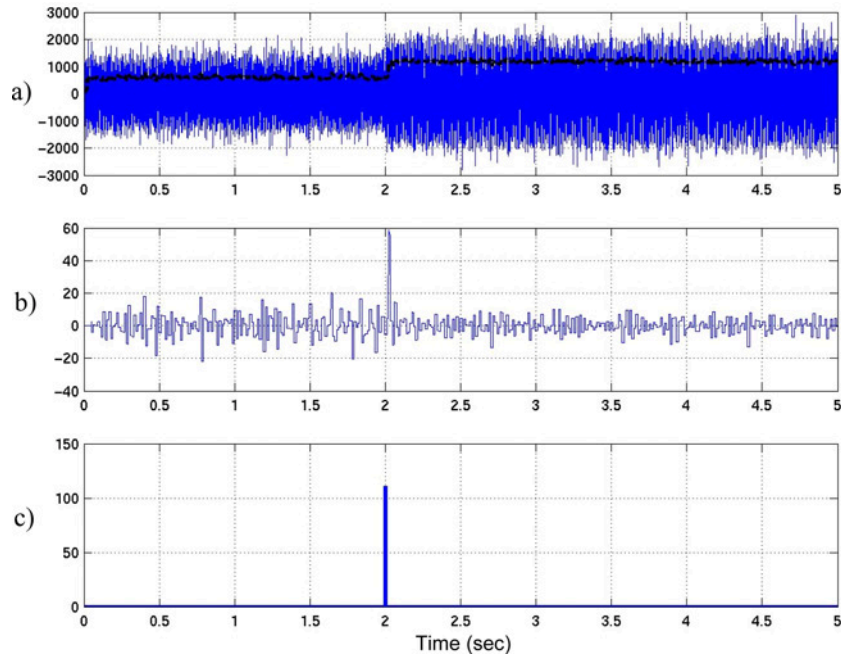


**Fig. 8** Vibration features extracted during a simulated FOD event at 2.0 seconds. a) Fan accelerometer signal with DFT-generated amplitude superimposed. b) Amplitude rate-of-change. c) “Wavelet Feature” produced by processing the signal through the algorithm shown in Fig. 6.

### III. Evidence Fusion Based On Imprecise Information

The majority of diagnostic system development utilizes simulated data, at least in the initial phases. For many components in the initial phase of design, the only dynamic data available are provided by simulation models. Even when actual data are available for diagnostic system development, the data many times are not acquired under in-service conditions. Thus the diagnostic system must be robust to model uncertainty as well as to uncertainties due to usage and off-design operation; it must provide a diagnosis based on imprecise information. The system should have the capability to fuse together multiple sources of evidence in order to enhance confidence in the diagnosis. Until recently many of these systems have utilized Bayesian-based probabilistic methods such as Bayesian Belief Networks and Bayesian Hypothesis Testing.<sup>16</sup> Use of a Bayesian method implies that the conditional probabilities required are determined via testing, i.e., the probabilities that observations made given the occurrence of certain events are based on actual data (or well-understood distributions presented in the literature) and precisely known. This many times is not the case due to the prohibitive costs of running the necessary tests or the rarity of the event. Indeed, as mentioned previously, the component may not even exist for the diagnostic system being designed. A means for reducing the available evidence, i.e., the features extracted from sensors via Kalman filters, or vibration signals described earlier, and developing a measure of the *possibility* of FOD occurrence is required. The output of the system will be imprecise as well, providing a range of probabilities (upper and lower bounds) in lieu of a crisp or exact output which, in the present context, could provide a misleading impression of the state of the system.

Data or sensor fusion is the process by which raw data are obtained from several sensors based in significantly different phenomenology observing the same event, and converted to a measure of how likely the event is to have occurred.<sup>27</sup> The measure may be the basis for a decision or may simply be for informational purposes. The fusion may be performed at the raw data level, feature level, or decision level, or combinations of each. Typically, raw data are reduced to a compact set of features, which provides an efficient means for expert diagnosis. The features are fused by an “expert,” in this case a fuzzy logic-based inference system,<sup>28,29</sup> into a diagnosis (opinion) based on the evidence available. Each expert’s opinion is in turn fused by combining the “weight of evidence” provided by each expert via an appropriate rule. Consider as an example the “gas path expert” shown in Fig. 9. The estimated fan efficiency

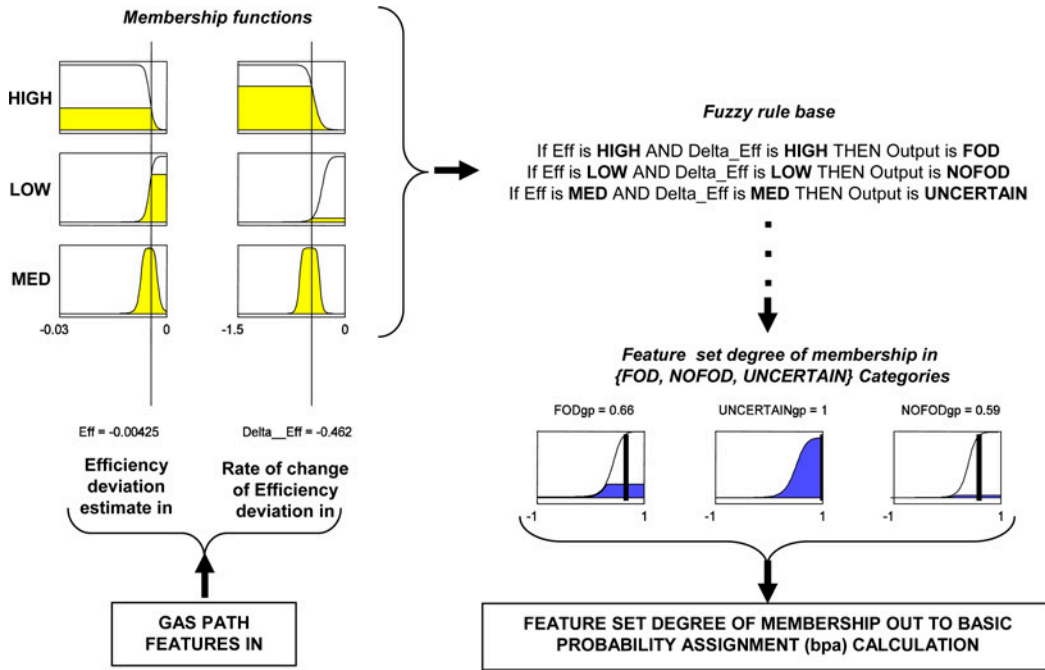


Fig. 9 Gas path expert membership functions and implication operations.

deviation and rate-of-change of efficiency deviation, i.e. features, are input into the set of fuzzy membership functions that categorize the evidence as indicating a low, medium, or high likelihood of FOD event occurrence. Each degree of membership is combined using a multiplicative AND operation, with the mean of maximum defuzzification operation providing a FOD, NOFOD, or UNCERTAING expert decision. Design of membership functions and aggregation rules is based on expert knowledge.<sup>29</sup> In a probabilistic decision setting, with say, the *a posteriori* probability of a FOD occurrence being determined via Bayes' law, a crisp probability of a FOD event,  $PROB(FOD)$ , would imply that  $PROB(NOFOOD) = 1 - PROB(FOD)$ . In the context of evidence theory however, there may be evidence that supports both propositions due to incomplete knowledge of the system. In the latter case, all of the possibilities must be accounted for and converted into "basic probability assignments" (bpa), also known as probability masses, which are essentially sets of probabilities which contain the actual probabilities. The output of the fuzzy aggregation rules therefore form a "possibility" distribution<sup>16,30,31</sup> from which the bpa  $m(\cdot)$  are determined, and obey a rule analogous to that required of crisp probabilities  $m(FOD) + m(NOFOOD) + m(UNCERTAING) = 1.0$ . Transformation from fuzzy degree of membership, to possibility assignment, to bpa is described in Ref. 31 and Ref. 32. The fuzzy inference engine for the gas path expert is shown in Fig. 9. For the vibration expert portion of the fusion, the same process is performed to arrive at the bpa. The vibration expert fuzzy inference engine is shown in Fig. 10.

The final step in the fusion requires combining the bpa provided by each expert. The original method used in evidence theory is Dempster's rule of combination<sup>16</sup>

$$m_{1,2}(A) = \frac{\sum_{A_i \cap A_j = A} m_1(A_1) \cdot m_2(A_2)}{1 - K} \quad (2)$$

for  $A \neq \emptyset$  and  $m_{1,2}(\emptyset) = 0$  and

$$K = \sum_{A_i \cap A_j = \emptyset} m_1(A_1) \cdot m_2(A_2)$$

The bpa  $m_i$  (aka *probability masses* or *belief structures*<sup>33</sup>) represent the degree or weight of evidence that supports a given proposition. In the present context the bpa are designated as  $m(FOD)$ ,  $m(NOFOOD)$ ,  $m(UNCERTAING)$ . Another

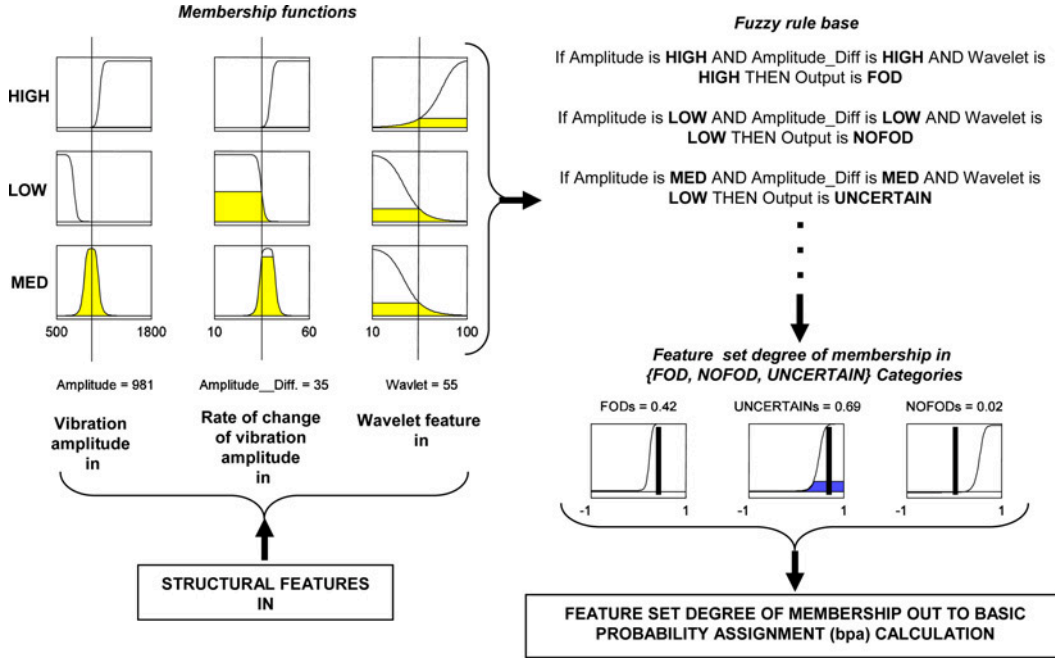


Fig. 10 Vibration expert membership functions and implication operations.

interpretation for the belief structure could be the proposition: “a FOD event has occurred. Given the evidence based on the features extracted from the data, the bpa are  $m(T)$ ,  $m(F)$ ,  $m(T,F)$ ,” i.e., some of the evidence supports that a FOD event has occurred, some that a FOD event has not occurred, and some supports either proposition. The subscripts denote the sources (or experts) assigning the weights to the evidence. There may be more than two sources. The factor  $K$  in the denominator of Eq. (2) is used to remove the effect of conflicting expert opinions, essentially ignoring the conflict, which, as Shafer points out<sup>34</sup> may result in an erroneous diagnosis. Dempster’s rule was later modified by Yager<sup>34</sup> to incorporate conflict among experts as additional uncertainty—removing the  $1 - K$  term in the denominator of Eq. (2) and adding  $K$  onto mass corresponding to the uncertain set. This provides a more prudent means for incorporating conflicting opinions which, in actuality, leads to decreased confidence (i.e., greater uncertainty) in the final decision.

Thus, after all modifications to the calculation as described above, the final bpa for the FOD application are:

$$\begin{aligned}
 m_{SE,GPE}(FOD) &= m_{SE}(FOD) \cdot m_{GPE}(FOD) + m_{SE}(FOD) \cdot m_{GPE}(UNCERTAIN) \\
 &\quad + m_{SE}(UNCERTAIN) \cdot m_{GPE}(FOD) \\
 m_{SE,GPE}(NOFOD) &= m_{SE}(NOFOD) \cdot m_{GPE}(NOFOD) + m_{SE}(NOFOD) \cdot m_{GPE}(UNCERTAIN) \\
 &\quad + m_{SE}(UNCERTAIN) \cdot m_{GPE}(NOFOD) \\
 m_{SE,GPE}(UNCERTAIN) &= m_{SE}(UNCERTAIN) \cdot m_{GPE}(UNCERTAIN) + K \\
 K &= m_{SE}(FOD) \cdot m_{GPE}(NOFOD) + m_{SE}(NOFOD) \cdot m_{GPE}(FOD)
 \end{aligned} \tag{3}$$

where the subscript  $SE$  stands for *Structural Expert*, and  $GPE$  stands for *Gas Path Expert*. The value of each of these bpa is computed at each time step, and the final values after the transient period of the actual suspected FOD event may be used to help make a decision.

In order to effectively process the features extracted, each with its own respective processing time delays and duration, the fusion algorithm requires that the features are provided to the fuzzy classifier in a *pseudo synchronous* fashion, i.e., the transient values of the features are “latched” at their maximum values in order to ensure that all of

the information is ultimately processed by the fusion. For the present study, a *fusion horizon*, the data window over which the fusion is performed, is five seconds. In an actual implementation, several overlapping data windows may be used to ensure adequate signal coverage for the event of interest.

#### IV. Evidence Fusion Applied to Simulated FOD Events

The data fusion process presented in Fig. 1 was applied to simulated data from a combined-effects gas path/vibration model of a large turbofan engine.<sup>15,35</sup> Three cases were simulated, which are described in Table 1.

It is important to realize that the gas path membership functions (Fig. 9) and structural membership functions (Fig. 10) are based strictly on the authors’ judgment, not on any test data nor analysis of a specific engine, and thus are fairly arbitrary, i.e., the classification values in this paper should not be considered descriptors of the likelihood of FOD damage in a real engine. The literature contains some quantitative information on gas path health after “moderate” and “severe” FOD events,<sup>8</sup> but there is no reasonable way to relate those to values the present work, given that this system is really meant to validate suspected FOD events. These examples should be viewed as demonstrations of how such a system would work, once it is configured for a particular engine. The power of this approach is that the membership functions can be easily tuned for a given engine, based on its size, structural dynamics, etc.

The simulation procedure is to run the gas path and structural models simultaneously to generate data such as would be obtained from a physical engine; the simulation models used here<sup>15,35</sup> produce responses that are representative of those a real engine would produce. A shift in fan efficiency is injected into Eq. (1) as shown in Fig. 3. Estimation of a health parameter shift using a Kalman filter as shown in Fig. 2 is a straightforward, well-established procedure. The abruptness and size of the step will influence the computed rate-of-change value. Once determined, these are the features that are fed into the gas path membership functions (Fig. 9). Simultaneously, the structural model is excited by the simulated impact of the object, which sets it vibrating. The rate-of-change of the amplitude of the vibration signal and the edge-detecting Wavelet Feature are determined from the simulated vibration signal with any additional permanent imbalance included as shown in Fig. 8. These features are then fed into the structural membership functions (Fig. 10). The outputs of the gas path and structural membership functions are converted into their respective bpa, updated at each time step. These are fused using the rules in Eq. (3) at each time step to obtain the combined evidence of FOD. The simulated events occur at cruise conditions under multivariable closed-loop control, demonstrating the fusion system’s ability to differentiate between conditions resulting purely from the FOD event and those due to the response of the controller.

Figure 11 through Fig. 13 each present the bpa determined by a) the vibration expert, b) the gas path expert, and c) the result of the fusion of the two using Yager’s modification to Dempster’s rule of combination. The results in Fig. 11 correspond to a simulated FOD-event occurring at 2 seconds due to a 0.5 lbm hard object hitting the fan blade at a relative speed of 300 mph at a radius of 20 inches. The simulated data were also used to calculate the gas path and vibration features shown in Fig. 3 and Fig. 8. As shown in the figure both experts consider the features observed to be conclusive evidence of FOD, with all of the probability mass assigned to  $m(\text{FOD})$  within one second of the event. The majority of the delay is due to the calculation of the fan efficiency estimate running average, required to provide a smooth rate-of-change feature calculation. The fluctuation observed in the bpa for the experts and fusion

**Table 1 Simulated FOD cases.**

	Gas Path Input	Structural Input
Case 1 (Fig. 11)	Efficiency deviation in the HIGH range (Fig. 9)	Impact causes Vibration amplitude in the HIGH range (Fig. 10) Additional permanent imbalance
Case 2 (Fig. 12)	Efficiency deviation in the MEDIUM range (Fig. 9)	Impact causes Vibration amplitude in the MEDIUM range (Fig. 10) Little additional permanent in balance
Case 3 (Fig. 13)	Efficiency deviation in the HIGH range (Fig. 9)	Impact causes Vibration amplitude in the LOW range (Fig. 10) No additional permanent imbalance

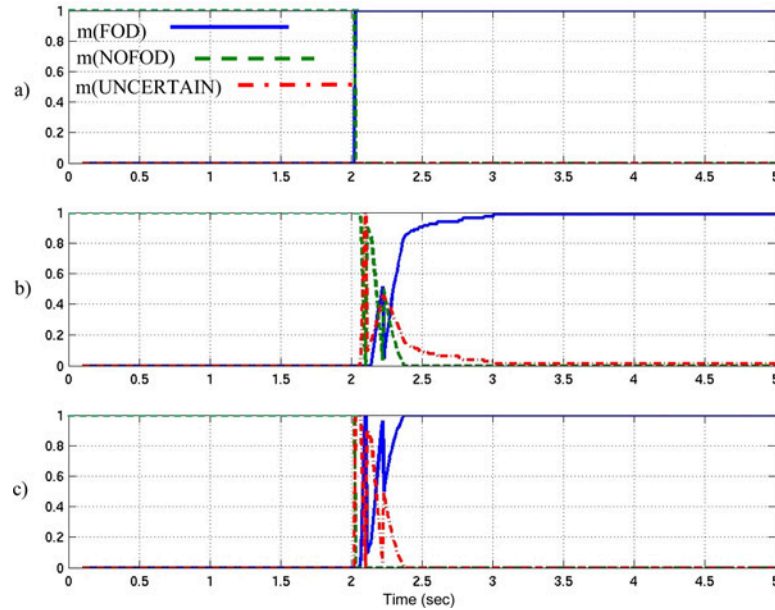


**Fig. 11 Basic probability assignments determined by a) the vibration expert, b) the gas path expert, and c) the fusion. Strong evidence supporting FOD.**

immediately after the event is due to the combined effect of noise and event severity on the fuzzy classification of the features. The fuzzy membership functions (shown in Fig. 9 and Fig. 10) are curves of various slopes, with regions of small and high slope depending on the values of the features. As the features transition from values corresponding to NOFOD (zero slope) to regions corresponding to FOD (again, zero slope), the larger slopes result in greater sensitivity to variations in the features, i.e., greater sensitivity to noise.

Figure 12 shows the fusion corresponding to a somewhat more benign FOD event. The foreign object hits the fan at the same position and speed as before, with a mass of 0.35 lbm. Neither expert commits to a decision regarding a FOD event, which is illustrated by the non-zero masses for the UNCERTAIN and NOFOD categories several seconds after the event. The structural expert provides somewhat less confidence than the gas path expert that a FOD event has occurred, and the fused  $m(\text{FOD})$  is slightly higher than for the two individual experts. Thus, from the point of view of the overall system, this can still be viewed as reinforcement since the experts agree that there is not enough evidence to declare that a FOD event has occurred. Even though no definitive answer is reached, this shows that the experts are in agreement on the limits of their ability to diagnose with confidence. The observed delay in arriving at the final fusion is primarily due to the effect of noise in the classification of the features (which, as described previously, would have a more pronounced effect for less significant events), the algorithm processing time, and the subsequent redistribution (recalculation) of the bpa. As shown in Fig. 8a, the final value of the vibration amplitude feature may be slightly affected by noise at times after the event has occurred. This may have a slight effect on the final fusion value; however the final value of the structural expert's bpa is overwhelmingly dominated by the change in amplitude due to the event, and to a much lesser extent, the noise.

Figure 13 presents the results of the fusion where there are conflicting opinions among the experts, i.e., the gas path analysis suggests that a FOD event has definitely occurred, while the features observed by the vibration expert indicate that there is virtually no evidence supporting the occurrence of a FOD event. Since shifts in health parameters may be caused by a variety of gas path faults, the gas path expert is merely indicating that, from its point of view, the symptoms of foreign object ingestion exist. This is not supported by the vibration expert.

The non-zero  $m(\text{UNCERTAIN})$  essentially indicates that it is *at least plausible* that a FOD event could have occurred. Thus, for example, the fusion output presented in Fig. 12 and Fig. 13 may be put in terms of the *Belief* that a FOD event has occurred,  $BE(\text{FOD})$ , and *Plausibility* that a FOD event could have occurred,  $PL(\text{FOD})$ , given the

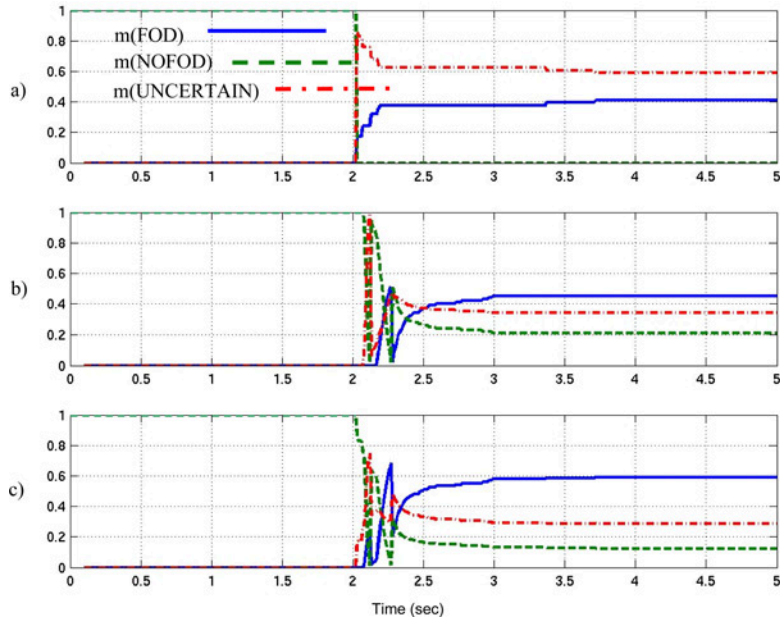


**Fig. 12 Basic probability assignments determined by a) the vibration expert, b) the gas path expert, and c) the fusion. Marginal evidence supporting FOD.**

evidence observed.  $BE(FOD)$  is defined as the mass resulting from evidence directly supporting FOD occurrence, i.e.,  $m(FOD)$ , while  $PL(FOD)$  is defined as the mass *not supporting*  $m(NOFOD)$ , i.e.,  $1 - m(NOFOD)$ . Figure 14 shows the evidence fusion of Fig. 12 and Fig. 13 in terms of the *belief* that a FOD event has occurred and the *plausibility* that a FOD event has occurred. The actual probability of FOD occurrence,  $PROB(FOD)$ , is bounded by the belief and

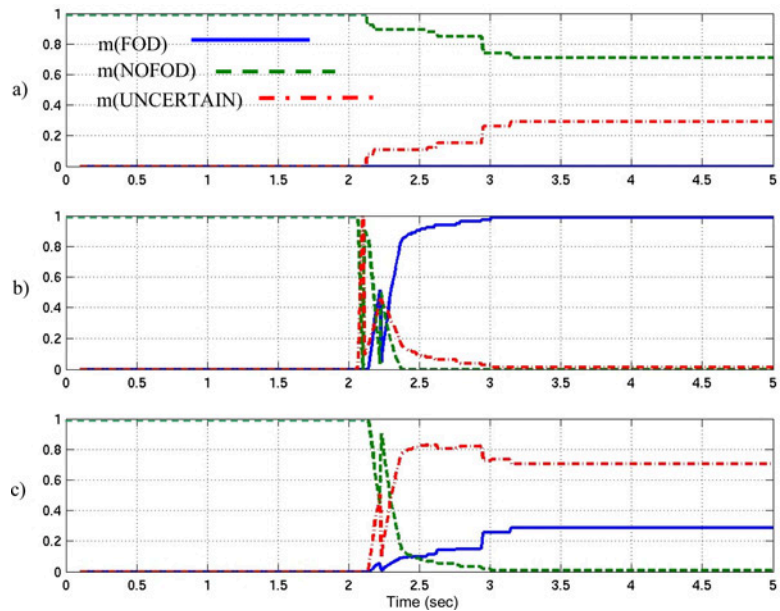


**Fig. 13 Basic probability assignments determined by a) the vibration expert, b) the gas path expert, and c) the fusion. Conflicting Evidence.**

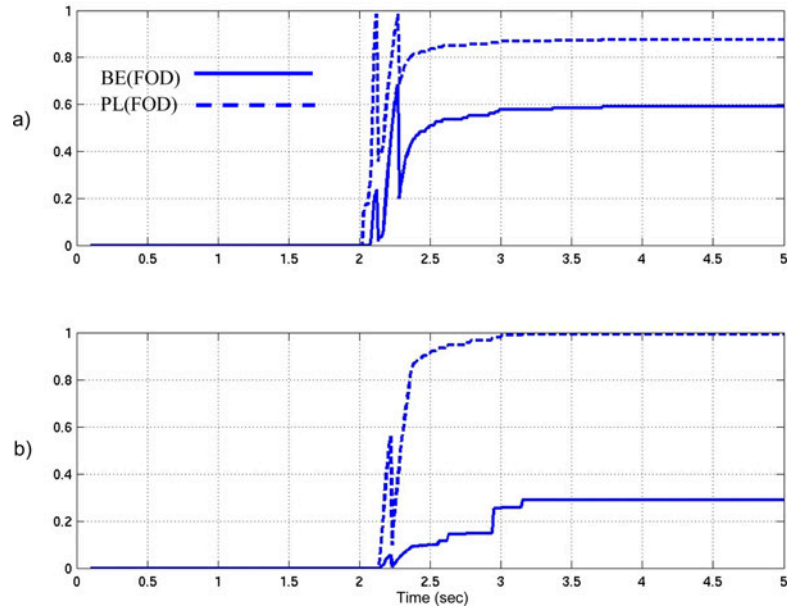


**Fig. 14** Post-fusion Plausibility and Belief functions for a) Marginal evidence supporting FOD (refer to Fig. 12), and b) Conflicting Evidence (refer to Fig. 13).

plausibility where  $BE(FOD)$  is considered to be the lower bound and  $PL(FOD)$  is considered to be the upper bound. Figure 14a might be interpreted to indicate that the likelihood of FOD is fairly high since both curves are not only similar but are also reasonably high. Figure 14b might suggest that the confidence in the occurrence of FOD is low due to the disagreement of the experts and subsequent low belief value  $BE(FOD)$ . This points out the need in a real implementation for a belief threshold that would trigger an action once it is exceeded. In the case where  $BE(FOD)$  equals  $PL(FOD)$ ,  $PROB(FOD) = PL(FOD) = BE(FOD)$ . Thus, one could say that the fusion shown in Fig. 11 results in  $PROB(FOD) = 1.0$ , i.e.,  $m(NOFOD) = 0.0$ ,  $PL(FOD) = 1 - m(NOFOD) = BE(FOD) = m(FOD) = 1.0$ .

### V. Conclusions

The FOD event data fusion system developed combines feature-based evidence from multiple sources, thereby making an assessment more reliable and enhancing confidence in a diagnosis. This system provides a feature-level fusion and does not provide a “crisp” diagnosis nor, for that matter, a policy for corrective action. The information set (i.e., the range of probabilities of FOD occurrence) provided by the feature-level fusion would be used by a decision-level fusion for diagnosis and corrective action depending on the policy adopted—neither of which is addressed in this paper.

The fusion is shown to provide a reliable assessment for two “experts” in agreement, i.e., where both see the evidence as strongly supporting the possibility of FOD occurrence. Where uncertainty or ignorance exists about the features being observed, the experts provide an uncertain assessment, with the uncertainty quantified by the plausibility and belief of occurrence (which would both be equal to 1.0 in the previous scenario). For situations where the fusion shows direct conflict among experts, i.e., one of the experts concludes that a FOD event has definitely occurred and the other concludes that a FOD event has not occurred, this uncertainty band may be quite large, with the results indicating that one (or more) of the sensors providing information may be malfunctioning. Although two sources, or “experts,” fed opinions into the fusion for the present investigation, more sources of opinion<sup>17</sup> (i.e., sources generating mass assignments based on categorization of the evidence) could easily be incorporated.

The effectiveness of the fusion system relies heavily on the design of the fuzzy classifier (i.e., the membership functions) which, as mentioned previously, is designed using expert knowledge. In the case of the present design, the designer was confident of what feature values (calculated based on simulation results) would constitute a high likelihood of a FOD event and a low likelihood of FOD event. The exact shape of the membership functions, which



dictate the performance (e.g., response characteristics) of the fusion algorithm at intermediate feature values, was at the discretion of the designer, and may not represent the optimal shape for the application considered. The membership functions may be easily adjusted to provide more accurate feature classification in the event that empirical data are available and analysis of the data suggests that a redesign is necessary.

The use of fuzzy inference techniques combined with the Dempster-Shafer-Yager Theory of Evidence provides a theoretical justification for drawing conclusions based on imprecise or incomplete data, which can be easily adapted to other applications. The method presented provides a prudent technique for decision making in situations where there is significant uncertainty beyond that which would be encountered using probabilistic methods, i.e., test data to support the generation of probabilities and probability distributions is not, nor ever will be, available and only “expert” opinions are available.

### Acknowledgments

The authors gratefully acknowledge the guidance provided by Dr. Chuck Lawrence, NASA Glenn Research Center Structures Division, for providing much needed expertise in turbofan engine rotor structural model development.

### References

- <sup>1</sup>Society of Automotive Engineers, “Uncontained Turbine Engine Rotor Events Data Period 1984 Through 1989,” SAE SP-1270, 1998.
- <sup>2</sup>Airplane Turbofan Engine Operation and Malfunctions Basic Familiarization for Flight Crews, [online report], URL: [http://www.faa.gov/certification/aircraft/engine\\_special\\_topics.htm](http://www.faa.gov/certification/aircraft/engine_special_topics.htm) [cited 12 May 2004].
- <sup>3</sup>Mattingly, J. D., Heiser, W. H., Pratt, D. T., Aircraft Engine Design, Second Edition, American Institute of Aeronautics and Astronautics, Reston, VA, 2002.
- <sup>4</sup>Eschenfelder, P., “Wildlife Hazards to Aviation,” ICAO/ACI Airports Conference, Miami, FL April 24, 2001.
- <sup>5</sup>Turbofan Engine Malfunction Recognition and Response Final Report, [online report], URL: [http://www.faa.gov/certification/aircraft/engine\\_special\\_topics.htm](http://www.faa.gov/certification/aircraft/engine_special_topics.htm) [cited 12 May 2004].
- <sup>6</sup>Grindle, T. J., Burcham, F. W., “Engine Damage to a NASA DC-8-72 Airplane from a High-Altitude Encounter with a Diffuse Volcanic Ash Cloud,” NASA/TM-2003-212030, August 2003.
- <sup>7</sup>Fisher, C. E., “Gas Path Debris Monitoring – a 21<sup>st</sup> Century PHM Tool,” 2003 IEEE Aerospace Conference, Big Sky, MT, March 18–25, 2000.
- <sup>8</sup>Kerr, L.J., Nemeč, T. S., and Gallops, G. W., “Real-Time Estimation of Gas Turbine Engine Damage Using a Control-Based Kalman Filter Algorithm,” Journal of Engineering for Gas Turbines and Power, Vol. 114, April 1992, pp. 187–195.
- <sup>9</sup>Luppold, R. H., Roman, J. R., Gallops, G. W., Kerr, L. J., “Estimating In-Flight Performance Variations Using Kalman Filter Concepts,” AIAA-89-2584, AIAA 25th Joint Propulsion Conference, Monterey, CA, July 10–12, 1989.
- <sup>10</sup>Klein, Lawrence A., *Sensor and Data Fusion Concepts and Applications*, 2nd Ed., SPIE Press Vol. TT35, 1999.
- <sup>11</sup>Doebelin, Ernest O., *Measurement Systems Application and Design*, 5th Ed., McGraw Hill Publishing, New York, 2004.
- <sup>12</sup>Kobayashi, T., Simon, D. L., “Application of a Bank of Kalman Filters for Aircraft Engine Fault Diagnostics,” Proceedings of the ASME Turbo Expo 2003, Power for Land, Sea, and Air, June 16–19, 2003, Atlanta, GA.
- <sup>13</sup>Lim, M. H., and Leong, M. S., “Diagnosis for Loose Blades in Gas Turbines Using Wavelet Analysis,” Proceedings of the ASME Turbo Expo 2003, Power for Land, Sea, and Air, June 16–19, 2003, Atlanta, Georgia.
- <sup>14</sup>Juluri, N., and Swarnamani, S., “Improved Accuracy of Fault Diagnosis of Rotating Machinery Using Wavelet De-Noising and Feature Selection,” Proceedings of the ASME Turbo Expo 2003, Power for Land, Sea, and Air, June 16–19, 2003, Atlanta, Georgia.
- <sup>15</sup>Turso, J., Lawrence, C., Litt, J., “Reduced-Order Modeling and Wavelet Analysis of Turbofan Engine Structural Response due to Foreign Object Damage (FOD) Events,” NASA/TM-2004-213118, 2004.
- <sup>16</sup>Thomopoulos, S. C. A., “Decision and Evidence Fusion in Sensor Integration,” *Control and Dynamic Systems*, Vol. 49, 1991.
- <sup>17</sup>Volponi, A. J., Brotherton, T., Luppold, R., Simon, D. L., “Development of an Information Fusion System for Engine Diagnostics and Health Management,” Proceedings of the 39<sup>th</sup> Combustion/27<sup>th</sup> Airbreathing Propulsion/21<sup>st</sup> Propulsion Systems Hazards/3<sup>rd</sup> Modeling and Simulation Joint Subcommittee Meeting, Joint Army-Navy-NASA-Air Force Interagency Propulsion Committee (JANNAF), Colorado Springs, Colorado, December 1–5, 2003.
- <sup>18</sup>Gelb, A. (Ed.), *Applied Optimal Estimation*, MIT Press, Cambridge, MA, 1999.
- <sup>19</sup>Volponi, A. J., “Sensor Error Compensation in Engine Performance Diagnostics,” ASME 94-GT-58, International Gas Turbine and Aeroengine Congress and Exposition, The Hague, Netherlands, June 13–16, 1994.
- <sup>20</sup>Simon, D., and Simon, D. L., “Kalman Filtering With Inequality Constraints for Turbofan Engine Health Estimation,” NASA/TM-2003-212111.

- <sup>21</sup>Adibhatla, S., Synk, E., Wiseman, M., "Model-Based Intelligent Digital Engine Control (MoBIDEC)," Air Force Research Laboratory, AFRL-PR-WP-TR-1998-2149, Wright-Patterson Air Force Base, OH 45433-7251, December 1998.
- <sup>22</sup>Ehrich, Fredric F., *Handbook of Rotordynamics*, Krieger Publishing Company, Inc., Malabar, FL, 1999.
- <sup>23</sup>Chan, Y. T., *Wavelet Basics*, Kluwer Academic Publishers, Boston, MA, 1995.
- <sup>24</sup>Abbate, A., DeCusatis, C., Das, P., *Wavelets and Subbands Fundamentals and Applications*, Birkhauser Publishing, Boston, USA, 2002.
- <sup>25</sup>Mallet, S., Hwang, W.L., "Singularity Detection and Processing With Wavelets," *IEEE Transactions on Info. Theory*, Vol. 38, No. 2, 1992.
- <sup>26</sup>Proakis, J.G., Rader, C.M., Ling, F., Nikias, C.L., *Advanced Digital Signal Processing*, Macmillan Publishing Co., New York, 1992.
- <sup>27</sup>Dempsey, P.J., Afjeh, A.A., "Integrating Oil Debris and Vibration Gear Damage Detection Technologies Using Fuzzy Logic," NASA/TM-2002-211126, NASA Glenn Research Center, Cleveland, OH, 2002.
- <sup>28</sup>*MATLAB Fuzzy Logic Toolbox User's Guide*, The Mathworks Inc., Natick, Mass, 2001.
- <sup>29</sup>Berkan, R., Trubatch, S., *Fuzzy Systems Design Principles Building Fuzzy IF-THEN Rule Bases*, IEEE Press, Piscataway, NJ, 1997.
- <sup>30</sup>Zadeh, L.A., "A Simple View of the Dempster-Shafer Theory of Evidence and its Implication for the Rule of Combination," *AI Magazine*, Summer, 1986.
- <sup>31</sup>Vachtsevanos, G., Kang, H., Cheng, J., Kim, I., "Detection and Identification of Axial Flow Compressor Instabilities," *Journal of Guidance, Control, and Dynamics*, Vol. 15, No. 5, 1992.
- <sup>32</sup>Yen, J., "Generalizing the Dempster-Shafer Theory to Fuzzy Sets," *IEEE Transactions on Systems, Man, and Cybernetics*, Vol. 20, No. 3, 1990.
- <sup>33</sup>Klir, G. J., Yuan, B., *Fuzzy Sets and Fuzzy Logic Theory and Applications*, Prentice Hall Publishing, Upper Saddle River, NJ, 1995.
- <sup>34</sup>Inagaki, T., "Interdependance Between Safety-Control Policy and Multiple-Sensor Schemes via Dempster-Shafer Theory," *IEEE Transactions on Reliability*, Vol. 40, No. 2, 1991.
- <sup>35</sup>Parker, K. I., and Guo, T.-H., "Development of a Turbofan Engine Simulation in a Graphical Simulation Environment," NASA-TM-2003-212543, August 2003.